超(超)临界火电机组 T91和 TP347H焊接性分析

郑 楷[1,2], 徐德生[3], 张雪莲[4], 谢 芳[4]
(1. 吉林大学 建设工程学院, 长春 130022; 2. 吉林建筑工程学院, 长春 130021;
3. 吉林大学 材料科学与工程学院, 长春 130025; 4. 珠海发电厂, 广东 珠海 519050)

摘 要: 通过珠海发电厂中港合资项目 1期工程 2×600 MW燃煤发电机组超临界压力和超 570 ℃高温的锅炉制造及安装, 在锅炉受热面中的再热器、过热器、省煤器和主蒸汽管路和联箱采用了国外生产的铁素体 SA213—T91(采用国家标准 GB5310—T91)和国外生产的奥氏体 SA213—TP347H耐热钢, 经分析阐述了两种耐热钢的金属特点和焊接性. 通过试验, 确定了 T91钢和 TP347H钢在锅炉生产和运行过程中产生裂纹、腐蚀、脆化等缺陷的主要因素. 有针对性的采取了相应的工艺措施, 进行了母材和焊接材料的工艺评定, 获得了优良的焊接接头. 有利于推广使用 T91和 TP347H耐热钢超(超)临界火电机组锅炉的制造.

关键词: 临界; T91; TP347H; 异种钢; 焊接
中图分类号: TG 44 文献标识码: A 文章编号: 0253—360X(2010)06—0053—03

郑 楷

0 序 言

火力发电在国内能源工业中具有特别重要的地位, 约占国内发电总量的 70%以上. 为了提高热效率, 减少 CO_2排放量, 适应环境和节约能源的要求, 世界各国都大力发展超(超)临界锅炉, 火电机组向大容量和高温高压高参数方向发展. 国内大容量高效率的超(超)临界机组近年来相继设计制造. 例如珠海电厂 2×600 MW超临界机组, 邹县及上海等电厂 1 000 MW超(超)临界机组均已投产运行. 按照标准规定和通常划分, 蒸汽压力≥22.11 MPa为超临界, 蒸汽压力≥30 MPa为超(超)临界发电机组. 随着火力发电机组容量的增大, 锅炉蒸汽压力和温度的上升, 使得锅炉的水冷壁、省煤器、再热器、过热器、主蒸汽管道及联箱管道等长期处于高温、高压以及氧化腐蚀恶劣条件下运行. 这就要求钢材具有较好的冶金质量和组织稳定性. 因而锅炉受热面必须采用强度更高、耐热性更好的高温材料. 焊接是现代火力发电机组锅炉制造、安装过程中最重要、工作量最大的加工工艺技术. 例如珠海发电厂超临界机组上述四管焊接焊口超过四万个. 焊接质量不合格, 焊口未焊透、夹渣、气孔、咬边、脆化、腐蚀、裂纹等缺陷是锅炉受热面爆漏的直接原因.

收稿日期: 2010—04—15
基金项目: 中港(李嘉诚)合资项目研究课题(广发(2004)1574)

1 T91和 TP347H焊接机理分析

中国超(超)临界火电机组异种钢焊接有两大类, 分别为铁素体(马氏体)与奥氏体钢接头, 铁素体与铁素体钢接头. 前者主要有 10Cr9Mo910/TP347H, 12Cr1MoV/TP347H, 钢 102(12Cr2MoWVTiB)/TP347H, T91/TP347H. 后者主要有 T91/12Cr1MoV, T91/钢 102等; 直径较大的主蒸汽管道也可采用 F11(X20CrMoWV121)或 F12与 12Cr1MoV铁素体与铁素体异种钢的焊接. T91与 TP347H的焊接适合超(超)临界火电机组锅炉的制造. 珠海电厂 2×600 MW超临界火电机组省煤器设计压力为 30.54 MPa, 再热器和过热器温度超过 570 ℃. 末级再热器材质为 SA213—TP347H, 出口过渡段管材为 SA213—T91(国家标准 GB5310). 过热器和省煤器也是锅炉最主要的承压部件之一, 所采用的材质与再热器基本相同. 再热、过热及省煤系统管径规格在 φ41.3 mm×φ6.04 mm到 φ457.2 mm×71.45 mm之间.

1.1 SA213—T91

T91(10Cr9Mo1VNb)钢属改良型 9Cr1Mo高强度马氏体耐热钢. 该钢种由美国首先研制. 由于它具有热强性好、强韧性高、导热性好、线膨胀系数小、价格低廉等原因广泛应用到超(超)临界锅炉的制造上. 但焊接极易出现裂纹、脆化等缺陷. 国内施工单位对 T91钢的焊接视为优先项目, 即焊接技术

通过后免除其它钢的焊接考核. 国内已开始生产(宝钢)该钢种. T91钢正火并经 730~770 ℃回火处理后,金属组织呈典型的马氏体骨架结构,导致 $M_{23}C_6$ 碳化物沉淀在马氏体骨架的边缘[1],如图 1 所示. 在较粗的 $M_{23}C_6$ 碳化物以及内部较细的沉淀转换成细箔之后,出现次微粒内较大的错位密度,这种细次晶粒结构是 T91钢高蠕变强度的决定因素. T91钢主要用于制造(亚)临界、超(超)临界、锅炉壁温≤625 ℃高温过热器、壁温≤650 ℃高温再热器,以及壁温≤600 ℃集箱和主蒸汽管道. T91的化学成分见表 1[4].

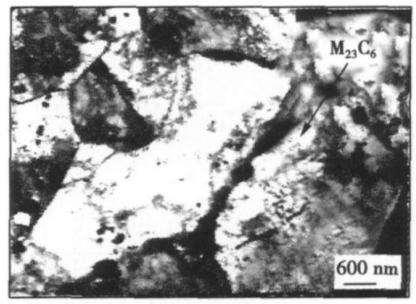

图 1 铁素体晶界碳化物(TEM像)

Fig. 1 Carbide in ferrite crystal boundary

表 1 T91钢的化学成分(质量分数,%)

Table 1 Chemical composition of T91 steel

	C	Si	Mn	P	S	Ni	Cr
SA213-T91	0.08~0.12	0.20~0.50	0.30~0.60	≤0.02	≤0.01	≤0.40	8.00~9.50
	Mo	V	Nb	Al	N	Fe	
SA213-T91	0.85~1.05	0.18~0.25	0.06~0.10	≤0.04	0.03~0.07	余量	

1.2 SA213—347H

SA213—347H属于 18—8型含铌稳定的奥氏体耐热不锈钢,相当于国内 1Cr19Ni11Nb钢,化学成分见表 2[5]. 这种钢有较好的抗晶间腐蚀性,较高的持久强度和抗氧化性,并且采取相应的措施也可获得较好的可焊性,因此主要用于制造临界、超(超)临界大容量火电机组锅炉. 珠海电厂 600 WM 超临界火电机组中的高压、高温过热器和再热器以及省煤器管路较大数量采用.

表 2 SA213-TP347H钢的化学成分(质量分数,%)

Table 2 Chemical composition of SA213-TP347H steel

C	Cr	Ni	Mn	Si
0.04~0.10	17.00~20.00	9.00~13.00	≤2.00	≤0.75
S	P	Nb	Fe	
≤0.030	≤0.040	0.06~0.10	余量	

1.3 T91与 SA213—TP347H焊接主要问题

根据焊接理论和实践分析,T91与 TP347H异种钢焊接存在的主要问题是焊缝裂纹、接头腐蚀以及脆化时效.

1.3.1 焊接裂纹

经过试验证明,主要是由于高温结晶过程产生的晶间裂纹. 当熔池中母材金属内的晶界上出现低熔共晶物(特别是低熔点硫化物熔点低于 900 ℃),金属结晶凝固后,晶界存在的低熔点共晶物仍是液态薄膜,此处受拉形成裂纹,这些裂纹与母材中的 C、S、P、N等元素含量有关,必须严格控制. 其次是结构应力和热应力造成的裂纹. 结构应力是由于结构刚度的约束和异种钢焊接接头线膨胀系数不一致以及强力组对形成的. 热应力的产生是壁厚的温差,即管件从室温到施焊时温度的升降整体不均匀造成的. 结构应力和热应力造成的焊接裂纹,通过有效的工艺措施及合理的结构设计避免.

1.3.2 焊接接头腐蚀

T91与 TP347H异种钢的焊接,与同类钢相比较细晶粒的 TP347H提高了耐蒸汽腐蚀作用. 这是由于钢中 Nb元素的加入,在焊接和热处理过程中 NbC的溶解与析出,使钢的晶粒细化,细晶粒加快了 Cr元素通过晶界的扩散,与氧形成一层细密的 Cr_2O_3 铬氧化层,Cr_2O_3 是防止钢生锈和蒸汽氧化腐蚀最重要的因素.

1.3.3 脆化失效

T91与 TP347H异种钢的焊接熔合,奥氏体在固溶状态具有良好塑性,Cr、Ni、Nb等元素逐渐以碳化物、金属化合物弥散析出,并向熔合区过渡,在固溶强化焊缝时使塑性和韧性降低. 这是脆化时效的倾向. 另外焊接材料和母材中 C元素含量增加,则使铁素体过饱和程度加强,也就是马氏体晶格变形加强,焊缝变脆,特别是当焊缝中 P和 H元素的存在使焊缝冷脆,严重时形成冷裂纹. 必须严格控制焊缝的含氢量,防止氢延迟裂纹,焊接缺陷引起应力集中产生冷裂纹,必要时实行消氢处理. 以上冷脆时效在焊接材料选择和焊接工艺措施加以控制.

2　焊接工艺

根据 T91与 TP347H异种钢焊接机理研究，在上述钢材进厂时，严格检验化学成分和力学性能，必须符合标准要求，焊接材料做工艺评定.

焊接质量与焊工技术操作控制焊缝金属的晶粒度关系很大. 每一次熔池凝固的晶粒在随后施焊被部分细化，这决定于每一道焊缝的宽厚以及焊接顺序，如图 2所示.

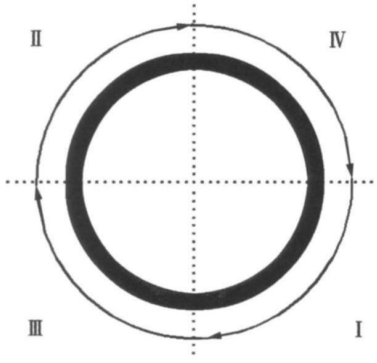

图 2　焊接顺序

Fig. 2　Welding sequence

焊前预热 200～250 ℃，层间温度低于马氏体转变温度（M_s）为 300～350 ℃. 在下一道焊接时热循环作用得到部分回火. 在热状态下施焊，焊后缓冷，冷却速度为 80 ℃/h改善了组织性能，减少了热应力.

薄壁管件可采用小电流无氢源的双层或三层 TIG焊，背部充氩保护，防止焊缝根部塌陷和氧化或过烧，厚壁件根部二层 TIG焊打底，焊条盖面. TIG焊焊丝采用 1Cr18Ni9Ti或镍基合金，盖面选用低氢型 R307焊条，有效控制了金属组织的稳定性和防止脆化.

焊后热处理过程为焊后冷却至 100～150 ℃保温时间 2 h后再进行 750～770 ℃回火处理后缓慢冷却，消除焊接残余应力和热应力，热影响区获得回火马氏体组织，如图 3所示，满足使用要求[1].

超临界火电机组异种耐热钢锅炉管排焊后，按照国家电力工业焊接技术标准进行焊缝表面质量检查，合格后全部进行无损 RT检测，个别无法进行 RT检测时，可用无损 PT检测代替珠海发电厂异种钢焊接接头一次探伤合格率超过 99%，焊缝表面如图 4所示.

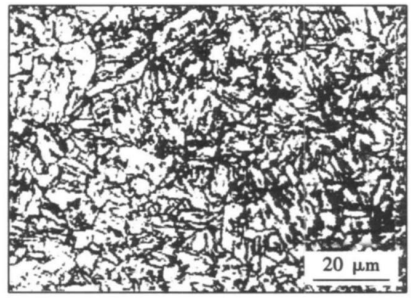

图 3　回火马氏体组织形貌

Fig. 3　Tempered martensite

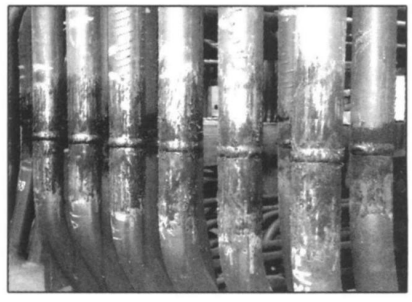

图 4　管排焊缝

Fig. 4　Tubes-line welding seam

3　结　　论

（1）T91与 SA213—TP347H异种钢焊接采取相应的工艺措施可获得抗裂、抗高温氧化腐蚀以及抗脆化时效性能均较好的焊接接头，适用于超（超）临界火电机组锅炉受热面过热、省煤及再热系统.

（2）为节约能耗，中国电力工业目前强制进行推（炸）掉 100 MW以下小火电机组，兴建容量 300 MW以上大型火电机组. 超（超）临界火电机组数量不断扩大，异种钢焊接的研究应落实到施工工艺规程中，使其规范化，提高超（超）临界锅炉的焊接质量.

参考文献：

[1]　束国刚，薛　飞，张　路，等. 国产化 P91钢工艺、组织和性能改进的研究[C]// 电力行业锅炉压力容器安全监督委员会. 超（超）临界锅炉用钢及焊接技术论文集. 北京：中国电力工业出版社，2005：14—17.

[2]　斯重遥，周振丰. 焊接手册[M]. 北京：机械工业出版社，1996.

[3]　金属材料编写组. 金属材料手册[M]. 北京：机械工业出版社，2002

[下转第 60页]

参考文献:

[1] Masubuchi Koichi. Analysis of Welded Structures[M]. London: Pergamon Press Ltd, 1980.

[2] 张建强, 张国栋, 赵海燕, 等. 铝合金薄板焊接应力三维有限元模拟[J]. 焊接学报, 2007, 28(6): 5—9.
Zhang Jianqiang, Zhang Guodong, Zhao Haiyan, et al. 3D-FEM numerical simulation of welding stress in thin aluminum alloy plate[J]. Transactions of the China Welding Institution, 2007, 28(6): 5—9.

[3] Zhu X K, Chao Y J. Effect of temperature-dependent material properties on welding simulation[J]. Computers and Structures, 2002, 80(11): 967—976.

[4] Matos P F P D, McEvily A J, Moreira P M G P, et al. Analysis of the effect of cold-working of rivet holes on the fatigue life of an aluminum alloy[J]. International Journal of Fatigue, 2007, 29(3): 575—586.

[5] Deng D. FEM prediction of welding residual stress and distortion in carbon steel considering phase transformation effects[J]. Materials and Design, 2008, 30(2): 359—366.

[6] Barsoum Z, Barsoum I. Residual stress effects on fatigue life of welded structures using LEFM[J]. Engineering Failure Analysis, 2008, 16(1): 449—467.

[7] 拉达伊 D. 焊接热效应[M]. 北京: 机械工业出版社, 1997.

[8] 武传松. 焊接热过程数值分析[M]. 哈尔滨: 哈尔滨工业大学出版社, 1990.

[9] 方洪渊. 焊接结构学[M]. 北京: 机械工业出版社, 2008.

[10] 关 桥. 关桥论著选编[M]. 北京: 北京航空制造工程研究所档案馆, 2002.

[11] Goldak J, Chakravarti A, Bibby M. A new finite model for welding heat source[J]. Metallurgual Transactions, 1984, 15B(2): 299—305.

[12] 陈翠欣, 李午申, 王庆鹏, 等. 焊接温度场的三维动态有限元模拟[J]. 天津大学学报, 2005, 38(5): 466—470.
Chen Cuixin, Li Wushen, Wang Qingpeng, et al. Three-dimensional dynamic FEM simulation of temperature distribution for welding process[J]. Journal of Tianjin University, 2005, 38(5): 466—470.

作者简介: 闫德俊, 男, 1978 年出生, 博士研究生. 主要从事焊接结构力学与疲劳寿命评估. 发表论文 3 篇.
Email: yandejun_2003@163.com

[上接第 55 页]

[4] 赵彦芬, 张 路, 赵林凤, 等. 国产 T91 钢在高温受热面中的应用评价[J]. 中国电力, 2009, 42(10): 5—11.
Zhao Yanfen, Zhang Lu, Zhao Linfeng, et al. Application evaluation of domestic T91 steel as high temperature boiler tube[J]. Electric Power, 2009, 42(10): 5—11.

[5] 章应霖. 奥氏体耐热钢和火电站异种钢管的焊接[C]// 电力行业锅炉压力容器安全监督委员会. 超(超)临界锅炉用钢及焊接技术论文集. 北京: 中国电力工业出版社, 2005: 57—60.

[6] 国家发展和改革委员会. DL/T869—2004 电力工业标准[S]. 北京: 国家标准出版社, 2004.

[7] 广东火电工程总公司. 焊接作业指导书[M]. 珠海: 广东火电工程总公司, 2006.

作者简介: 郑 楷, 女, 1976 年出生, 博士研究生, 讲师. 主要从事基础理论和专业理论的教学及研究工作. 发表论文 10 余篇.
Email: xudk@jlu.edu.cn

surface which the boiler withstands the supercritical pressure and the ultra 570 ℃ high temperature in manufacture and installment first phase 2×600 MW coal-fired generating units in China-HK (Hong Kong) joint project through the Zhuhai Power plant. The metal characteristics and welding performance of the two kind steels are analyzed and the primary factors of producing crack corrosion and embrittlement flaw in the boiler production and the movement process are determined by experiments and the craft evaluation of the parent metal and the welding material has carried out by using the corresponding craft measure. The fine weld joints are obtained which will promote the using of the T91 and TP347H heat-resistant steel in the manufacture of the promotion (ultra) supercritical pressure thermal power unit boiler.

Key words: critical; T91; TP347H; heterogenic steel; weld

Effect of thermophysical parameters on the hump feature of welding residual stress by finite element analysis YAN De-jun, LIU Xue-song, YANG Jian-guo, FANG Hong-yuan (State Key Laboratory of Advanced Welding Production Technology, Harbin Institute of Technology, Harbin 150001, China). p 56—60

Abstract: Numerical simulation of TIG welding of thin plate by thermo-elastic finite element method (FEM) was conducted. By double ellipsoid thermal source, thermophysical parameters varying with temperature were used to compare the influence of heat conductivity, specific heat capacity and density on the welding residual stress. The result shows that the drop of the heat conductivity will lead to the increment of the welding residual stress, and the longitudinal residual stress transits from the double hump to the single one; the falling of the specific heat capacity can also reduce the welding residual stress, which can greatly be affected by the difference of density between aluminum alloy and mild steel, and the double hump of the longitudinal residual stress will disappear with the density increasing. Then the three thermo-physical parameters, heat conductivity, specific heat capacity and density, make the longitudinal welding residual stress of aluminum alloy is lower than its yield limit and appears double hump effect near the weld seal. The welding longitudinal residual stress for the flat plates of 2024-T4 aluminum alloy is simulated by using cutting pieces stress relieving method. The simulation results are well accordant with the test ones, which prove the validity of the simulation results.

Key words: numerical simulation; longitudinal residual stress; thermophysical parameters; double hump effect

Establishment of relation about welding residual stress between simulative component and practical component on basis of similitude principles JI Shu-de, ZHANG Li-gui, LI Ya-fan, LIU Xue-song, FANG Hong-yuan (1. School of Aerospace Engineering, Shenyang Institute of Aeronautical Engineering, Shenyang 110034, China; 2. State Key Laboratory of Advanced Welding Production Technology, Harbin Institute of Technology, Harbin 150001, China). p 61—64

Abstract: On basis of the similitude principles, the conception of virtual simulative component and the auxiliary value of welding residual stress are deduced by the welding conduction theory, and the relation of the welding residual stress between the simulative component and the practical component is attained. Moreover, the welding experiment about the simulative plane and the practical plane proves the correctness of the relation, which the proportionality coefficient of dimensions between the simulative plane and practical plane is 1∶1.5. This provides a new idea to predict the welding stress distribution of large practical structure by the contractible physical model and has owns important theory meaning and practical engineering significance.

Key words: similitude principles; conduction theory; simulative component; welding residual stress

Numerical simulation on electron beam deep penetration welding and weld appearance of magnesium alloy LUO Yi-[2,3], LIU Jin-he, YE Hong, SHEN Bin[2] (1. School of Material Science and Engineering, Northwestern Polytechnical University, Xi'an 710072, China; 2. Province Key Laboratory of Advanced Welding Technology, Jiangsu University of Science and Technology, Zhenjiang 212003, Jiangsu, China; 3. School of Material Science and Engineering, Chongqing Institute of Technology, Chongqing 400050, China). p 65—68

Abstract: The numerical simulation on vacuum electron beam deep penetration welding for AZ61 magnesium alloy sheet with 10 mm thickness was studied. In view of the thermal effect about metal steam plasma and keyhole deep penetration during vacuum electron beam welding, the moving heat source model composed by Gauss surface source and double ellipsoid body source was developed. And the characteristics of thermal cycle and weld appearance under different welding processes were studied on the basis of simulation and experiment values. The results of simulation and experiment show that the composite source model can gain the effect of deep penetration of electron beam welding and calculate the temperature distribution and the weld geometry under the action of electron beam source. The results also prove that the model is applicable to the thermal effect simulation on the electron beam welding of AZ61 magnesium alloy sheet.

Key words: magnesium alloy; electron beam welding; composite heat source; weld appearance; numerical simulation

Effect of heat input on microstructure and low temperature impact resistance of welded joint of 9Ni steel Menggen-bagen[1,2], MA Cheng-yong, PENG Yun, TIAN Zhi-ling, LIN Wen-guang (1. College of Materials Science and Engineering, Inner Mongolia University of Technology, Huhhot 010051, China; 2. Central Iron & Steel Research Institute, Beijing 100081, China). p 69—72

Abstract: 9Ni steel was welded with submerged arc welding process, and the microstructure and fracture appearance of welded joints were analyzed. The effect of heat input on the microstructure and low temperature impact resistance of the joints was studied. The results show that with the increase of the heat input, dendritic segregation and precipitation phase in the weld reduce, and fracture dimples become larger and deeper, which make the impact resistance of the joints increase. The joints in different input can meet application requirements, which impact absorbing energy is superior to standard at -196 ℃ and hardness is inferior to 400 HV. The experiment results can be used as theoretic basis for making welding procedure of 9Ni steel.

Key words: 9Ni steel; heat input; welded joint; micro-